Environmental Science & Technology

pubs.acs.org/est

Article

Interspecies Differences in Activation of Peroxisome Proliferator-Activated Receptor γ by Pharmaceutical and Environmental Chemicals

Clémentine Garoche,* Abdelhay Boulahtouf, Marina Grimaldi, Barbara Chiavarina, Lucia Toporova, Marjo J. den Broeder, Juliette Legler, William Bourguet, and Patrick Balaguer*

Cite This: *Environ. Sci. Technol.* 2021, 55, 16489−16501

Read Online

ACCESS | Metrics & More | Article Recommendations | Supporting Information

ABSTRACT: Endocrine disrupting chemicals (EDCs) are able to deregulate the hormone system, notably through interactions with nuclear receptors (NRs). The mechanisms of action and biological effects of many EDCs have mainly been tested on human and mouse but other species such as zebrafish and xenopus are increasingly used as a model to study the effects of EDCs. Among NRs, peroxisome proliferator-activated receptor γ (PPARγ) is a main target of EDCs, for which most experimental data have been obtained from human and mouse models. To assess interspecies differences, we tested known human PPARγ ligands on reporter cell lines expressing either human, mouse, zebrafish, or xenopus PPARγ. Using these cell lines, we were able to highlight major interspecies differences. Known hPPARγ pharmaceutical ligands modulated hPPARγ and mPPARγ activities in a similar manner, while xPPARγ was less responsive and zfPPARγ was not modulated at all by these compounds. On the contrary, human liver X receptor (hLXR) ligands GW 3965 and WAY-252623 were only active on zfPPARγ. Among environmental compounds, several molecules activated the PPARγ of the four species similarly, e.g., phthalates (MEHP), perfluorinated compounds (PFOA, PFOS), and halogenated derivatives of BPA (TBBPA, TCBPA), but some of them like diclofenac and the organophosphorus compounds tri-*o*-tolyl phosphate and triphenyl phosphate were most active on zfPPARγ. This study confirms or shows for the first time the h, m, x, and zfPPARγ activities of several chemicals and demonstrates the importance of the use of species-specific models to study endocrine and metabolism disruption by environmental chemicals.

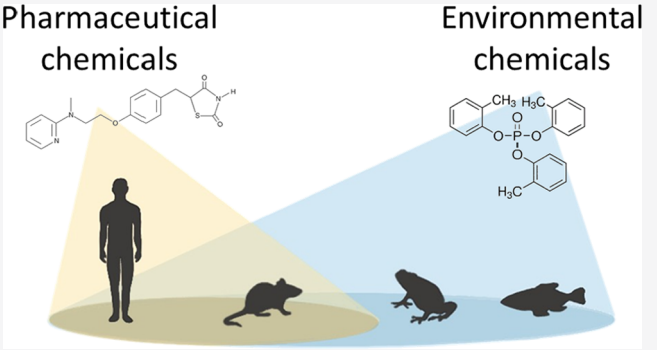

KEYWORDS: *peroxisome proliferator-activated receptor γ, zebrafish, luciferase reporter cell lines, pharmaceutical and environmental ligands*

INTRODUCTION

Nuclear receptors (NRs) are a family of transcription factors involved in the gene regulation of key physiological processes. Among NRs, the peroxisome proliferator-activated receptors (PPARs) are the target of fatty acids, eicosanoids (prostaglandins, leukotrienes), and vitamin B3 notably, and they are involved in the regulation of glucose, lipid, and cholesterol metabolism. PPARs act as heterodimers with the retinoid X receptors (RXRs) that bind to peroxisome proliferator response elements (PPREs), which are specific regions on the DNA of target genes, and once activated by a ligand modulate their transcription.

There are three known subtypes in the human (h) PPAR family, namely, hPPARα, hPPARβ/δ, and hPPARγ (NR1C1, NR1C2, and NR1C3, respectively), which are expressed in different tissues and play different roles.[1−4] hPPARγ is expressed at low levels in many tissues including muscles, colon, kidney, and pancreas and is highly expressed in adipocytes where it is involved in the regulation of lipid storage and adipogenesis.[5−10] Given this role, many synthetic hPPARγ ligands have been developed for the treatment of hyperlipidemia and diabetes such as thiazolidinediones including rosiglitazone and troglitazone.[11,12]

Because of the involvement of hPPARγ in important physiological processes and its potential implication in metabolic disorders such as diabetes and obesity, it is important to assess the ability of chemical substances present in the environment to interfere with this specific nuclear receptor. It has been shown that hPPARγ can be a target of

Received: June 29, 2021
Revised: November 10, 2021
Accepted: November 12, 2021
Published: November 29, 2021

https://doi.org/10.1021/acs.est.1c04318
Environ. Sci. Technol. 2021, 55, 16489−16501

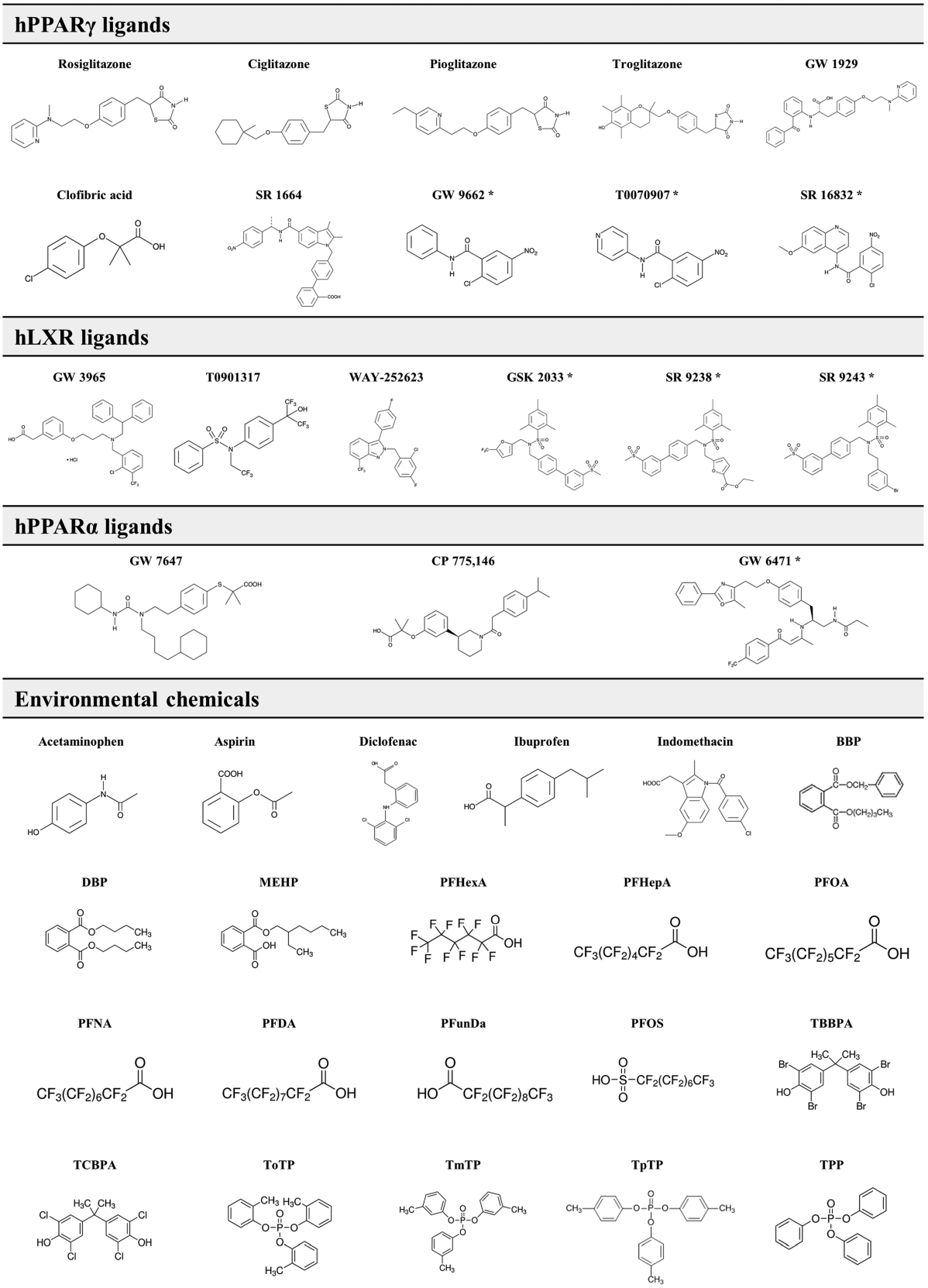

Figure 1. Chemical structures of the molecules used in this study. * NRs antagonists.

endocrine disrupting chemicals (EDCs), potentially resulting in an alteration of these processes, but most of the data have been produced using human and mouse models. In the past decade, zebrafish and xenopus models have been increasingly used as *in vivo* models to evaluate the impact of environmental compounds on organisms.[13−17] Nowadays, zebrafish is often used to study adipogenesis and metabolic diseases as the morphology of white adipose tissue is similar to human, and

https://doi.org/10.1021/acs.est.1c04318
Environ. Sci. Technol. 2021, 55, 16489−16501

pathways involved in lipid metabolism are highly conserved between mammals and fish.[18−20] Importantly, there is a lack of information regarding the interspecies differences in PPARγ activation as the data obtained from xenopus and zebrafish (aquatic) models might not be relevant to assess the endocrine disrupting potency of chemicals to humans. Conversely, natural and synthetic chemical substances could be released into the aquatic environment and target PPARγ of these species in a way that could not be extrapolated from human or mouse data.

To better assess interspecies differences, we tested a selection of synthetic and environmental hPPARγ chemicals on human, mouse, zebrafish, or xenopus PPARγ reporter cell lines. We used HeLa cells expressing luciferase under the control of five GAL4 response elements and the yeast GAL4 DNA-binding domain fused to the human, mouse, zebrafish, or xenopus PPARγ ligand-binding domain.[18,21] The findings of the current study provide new information about the relevance of using *in vivo* animal assays for evaluating the toxicological risk posed by EDCs on humans, fishes, and wildlife.

MATERIALS AND METHODS

Chemicals. Molecules tested in this study and their chemical structure are presented in Figure 1 and Supplementary Table 1. All of the chemicals were obtained from Sigma-Aldrich Chemical Co. (Saint-Quentin Fallavier, France). Stock solutions of chemical substances were prepared in dimethyl sulfoxide (DMSO) and stored at −20 °C. Fresh dilutions of test chemicals in culture medium were prepared before each experiment, and the final DMSO concentrations did not exceed 0.1% (v/v) of the culture medium.

Reporter Cell Lines. The luciferase reporter gene cell lines were established in two steps. The HG5LN cell line was generated by transfecting HeLa cells with the p(GAL4RE)5-β-globin-Luc-SV-Neo plasmid containing a luciferase reporter gene driven by a pentamer of the yeast activator GAL4 recognition sequence in front of the β-globin promoter and a neomycin phosphotransferase gene under the control of SV40 promoter. The HG5LN-hPPARγ,[21] -mPPARγ, -zfPPARγ,[18] and -xPPARγ cell lines were obtained by transfecting HG5LN cells with the pSG5-GAL4(DBD)-PPARγ (LBD)-puro plasmid so that they express a chimeric protein containing the yeast transactivator GAL4 DNA-binding domain (DBD) (M1-S147) fused to ligand-binding domain (LBD) regions of human (S204-Y505), mouse (S204-Y505), xenopus (K171-Y477), or zebrafish (K213-Y527) PPARγ. The HG5LN-hLXRα, -hLXRβ, and zfLXR cell lines (Toporova et al., 2020) were obtained by transfecting HG5LN cells with the pSG5-GAL4(DBD)-LXR (LBD)-puro plasmids. For each receptor, 5−10 clones were chosen for their ligand-induced luciferase expression. The clones were amplified, and luciferase expression was checked at several passages. For each receptor, the clone with the best induction of luciferase activity was selected and used for the screening of the different chemicals. The stability and the inducibility of luciferase expression were checked during at least 20 passages (20 weeks). We also measured the expression of the different GAL4 fusion proteins by RT-PCR expression using GAL4-DBD-specific primers (forward: 5′-ACG GCA TCT TTA TTC ACA TT-3′, reverse: 5′-CGA ACA AGC ATG CGA TAT TT-3′) to confirm that the different Gal4-PPAR fusion proteins were expressed at similar levels (data not shown).

Cell Culture Conditions. HG5LN cells were grown in Dulbecco's modified Eagle's medium: nutrient mixture F-12 (DMEM/F-12) with phenol red, supplemented with 10% fetal bovine serum (FBS), 1% penicillin/streptomycin, and 1 mg/mL G418 in a 5% CO_2-humidified atmosphere at 37 °C. HG5LN-PPARγ and -LXR cell lines were cultured in the same medium supplemented with 0.5 μg/mL puromycin.

Exposures with pharmaceutical and synthetic chemicals were made in phenol red-free DMEM/F-12 medium supplemented with 5% dextran-coated charcoal (DCC)-treated FBS and 1% penicillin/streptomycin. As some of the environmental chemicals, such as TBBPA, can strongly bind proteins present in the serum of the culture medium, exposures of environmental chemicals were made in the absence of serum. The test medium was phenol red-free DMEM/F-12 medium, 1% penicillin/streptomycin, and 1% pluronic acid.

***In Vitro* Transcriptional Activation Bioassay.** Cells were seeded in 96-well white opaque culture plates (Greiner bio-one 655083-905 CellStar; Dutscher, Brumath, France) at a density of 50 000 cells per well in 150 μL culture medium. After 24 h, the culture medium in the plates was replaced with 200 μL test medium containing tested chemical compounds at different concentrations or solvent control (DMSO; 0.1% v/v) in quadruplicates. Activities are expressed as a percentage of the maximal luciferase activity induced by 1 μM rosiglitazone (HG5LN-hPPARγ, HG5LN-mPPARγ), 10 μM GW 3965 (HG5LN-zfPPARγ), or 10 μM rosiglitazone (HG5LN-xPPARγ). For antagonist assays, tested compounds were coexposed with the reference compound at a concentration yielding 60−80% of the maximum luciferase activity, i.e., 30 nM rosiglitazone (HG5LN-hPPARγ, HG5LN-mPPARγ), 2.6 μM GW 3965 (HG5LN-zfPPARγ), or 2 μM rosiglitazone (HG5LN-xPPARγ). The identified chemicals were tested at different concentrations of the reference agonist compound to prove that they are competitive inhibitors (data not shown).

Environmental compounds were tested without serum and with 1% pluronic acid, with activities expressed as a percentage of the maximal luciferase activity induced by 1 μM rosiglitazone (HG5LN-hPPARγ, HG5LN-mPPARγ), 3 μM GW 3965 (HG5LN-zfPPARγ), or 10 μM rosiglitazone (HG5LN-xPPARγ). Plates were then incubated at 5% CO_2 ± 37 °C for 24 h. At the end of the incubation, the medium was replaced with 50 μL per well of medium containing 0.3 mM D-luciferin. Luminescence signal was measured in living cells for 2 s per well using a MicroBeta Wallac luminometer (PerkinElmer). Each compound was tested in at least three independent experiments. To assess whether the modulation of luciferase activity in our models was indeed mediated by PPARγ, the active chemical substances were also tested on the HG5LN parental cell line, which expresses only the GAL4-driven reporter gene and should not be activated by PPARγ ligands.

Data Analysis. Results are expressed as the percentage of the maximum luciferase activity induced by the reference ligand for each cell line, i.e., 1 μM rosiglitazone (HG5LN-hPPARγ, HG5LN-mPPARγ), 10 μM GW 3965 (HG5LN-zfPPARγ), and 10 μM rosiglitazone (HG5LN-xPPARγ). Individual agonist dose−response curves, in the absence and presence of antagonist, are fitted using the sigmoidal dose−response function of a graphics and statistics software program (GraphPad Prism 6, GraphPad Software Inc.). Effective concentrations (ECs) and inhibitory concentrations (ICs) are derived from the Hill equation. For a given chemical, EC_{50}

https://doi.org/10.1021/acs.est.1c04318
Environ. Sci. Technol. 2021, 55, 16489−16501

is defined as the concentration inducing 50% of its maximal effect and IC_{50} represents the concentration required for 50% inhibition. The EC_{50s} were calculated taking into account the basal activity of each cell line and constraining the top as the maximum activity of the tested chemical and the bottom as the basal activity of the cell line. For antagonism assays, the top was constrained as the percentage obtained with the antagonism control (at the concentration yielding 60−80% of the maximum luciferase activity) and the bottom was constrained at the minimum plateau reached by the tested chemical.

As the basal luciferase expression in the hPPARγ cell lines is 11% of the maximal expression, the induction factor of the reference ligand is 9.1. A *z*-factor was calculated and is 0.7, indicating that the risk of overlap between negative and positive controls is negligible, as a good *z*-factor should be in the [0.5−1] range. For the mPPARγ cell line, the basal luciferase expression is 15% and thus the induction factor of the reference ligand is 6.7. The *z*-factor is 0.7. For the zfPPARγ cell line, the basal luciferase expression is 6% with an induction factor of 16.7 and a *z*-factor of 0.8. For the xPPARγ cell line, the basal luciferase expression is 8% with an induction factor of 12.5 and a *z*-factor of 0.9.

Molecular Modeling. The various docking models were generated with the server EDMon (http://edmon.cbs.cnrs.fr) using the default parameters. The PDB files of the ligands were generated from SMILES strings using the Grade web server (http://grade.globalphasing.org) and converted into mol2 files using Openbabel (http://www.cheminfo.org/Chemistry/Cheminformatics/FormatConverter/index.htm).

RESULTS AND DISCUSSION

Interspecies PPARγ Activity of Synthetic Ligands of hPPARγ. To ensure that chemicals did not modulate luciferase expression in a non-nuclear receptor-mediated manner, which could be interpreted as a false-positive result, all of the chemicals were tested in the HG5LN parental cell line. Nonspecific-induced activity was observed for some chemicals (SR 16832, DBP) at the highest tested concentrations in the HG5LN cells (Supplementary Figure 1A,B). Decrease of luminescence was also observed for other chemicals (SR 1164, diclofenac, PFunDA, and TBBPA) and could be the result of either toxicity or nonspecific inhibition of luciferase expression. As a result, the concentration ranges tested in the HG5LN GAL4-PPARγ reporter cell line transactivation assays were adjusted to exclude concentrations presenting nonspecific modulation of the luciferase expression.

To assess potential interspecies differences in the transactivation of hPPARγ, mPPARγ, zfPPARγ, and xPPARγ, we tested 10 known pharmaceutical and synthetic ligands of hPPARγ on the four reporter cell lines. The reference hPPARγ ligand rosiglitazone was an agonist for both hPPARγ and mPPARγ with close EC_{50} of 24 and 16 nM, respectively (Figure 2 and Table 1), which concurs with the literature.[11,18,22] This compound was hence used as the reference ligand in both cell lines with a maximum luciferase activity of 100% at 1 μM. In HG5LN-xPPARγ cells, rosiglitazone was also active but with less potency as its EC_{50} was 718 nM. Rosiglitazone was used as the reference ligand in this cell line with a maximum luciferase activity of 100% at 10 μM. As previously shown,[18] rosiglitazone had no agonistic nor antagonistic effect on zfPPARγ as it did not modulate luciferase expression in HG5LN-zfPPARγ cells (Figure 2 and Tables 1 and 2).

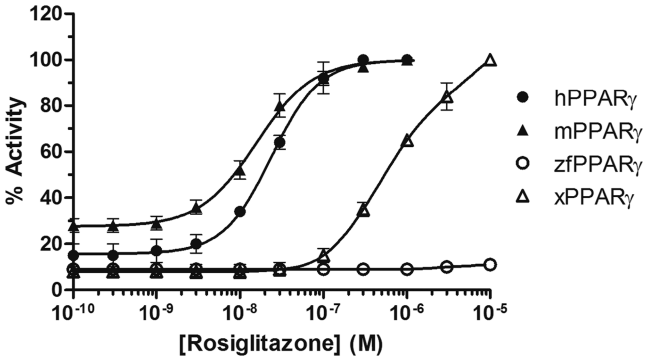

Figure 2. Transcriptional activity of h, m, zf, and xPPARγ in response to rosiglitazone. Results are expressed as a percentage of the maximum luciferase activity induced by 1 μM rosiglitazone (HG5LN-hPPARγ, HG5LN-mPPARγ), 10 μM GW 3965 (HG5LN-zfPPARγ), or 10 μM rosiglitazone (HG5LN-xPPARγ). Error bars represent standard deviations.

Other compounds of the thiazolidinedione class of antidiabetic drugs that were tested are ciglitazone, pioglitazone, and troglitazone, which all had profiles similar to rosiglitazone with lower potency and different efficacies and were also not able to activate nor inhibit zfPPARγ (Table 1).

GW 1929 is a known nonthiazolidinedione activator of hPPARγ. Indeed, GW 1929 was able to induce luciferase activity in HG5LN-hPPARγ, HG5LN-mPPARγ, and HG5LN-xPPARγ, displaying a slightly lower efficacy (81−85%) and better potency than rosiglitazone with EC_{50} 4−13 times lower (Figure 3A and Table 1). Similarly to rosiglitazone, GW 1929 was not an agonist nor an antagonist of zfPPARγ (Figure 3A, Table 1, and Supplementary Figure 1A,B).

Clofibric acid, a metabolite of the cholesterol-lowering pharmaceutical drug clofibrate, was able to transactivate hPPARγ, mPPARγ, and xPPARγ up to 39% (Table 1) but had no effect on zfPPARγ. No antagonist effect on any of the receptors was measured (Table 2).

Surprisingly, SR 16832, despite being described as a hPPARγ antagonist in the literature, was a very potent agonist on hPPARγ, mPPARγ, and xPPARγ. SR 16832 was even more potent than rosiglitazone with EC_{50} comprised between 0.3 and 1.0 nM on hPPARγ, mPPARγ, and xPPARγ (Table 1). However, this compound had no agonistic nor antagonistic activity toward zfPPARγ.

The hPPARγ antagonists GW 9662 and T0070907 were both antagonists in our human, mouse, and xenopus models with IC_{50} in the nM range (Table 2). Moreover, T0070907 was able to downregulate basal luciferase activity when tested alone on hPPARγ and mPPARγ, thus behaving as an inverse agonist of the PPARγ of these species as previously described[23] (Figure 3B). Interestingly, both compounds were partial agonists of xPPARγ with similar EC_{20s} in the nM range and a maximum of 41% for GW 9662 and 49% for T0070907 (Table 1). Finally, GW 9662 and T0070907 did not activate nor inhibit zPPARγ (Figure 3C).

The antidiabetic drug SR 1664[24] slightly transactivated hPPARγ and mPPARγ (up to 33%) with similar EC_{20s} but not xPPARγ nor zfPPARγ. A slight antagonism was observed in the four cell lines with a lower potency in HG5LN-xPPARγ and -zfPPARγ cells (Table 2).

https://doi.org/10.1021/acs.est.1c04318
Environ. Sci. Technol. 2021, 55, 16489−16501

Table 1. Maximal Activity and Half-Maximal Effective Concentration (EC_{50}) of the Pharmaceuticals and Synthetic Ligands on h, m, zf, and xPPARγ[a,b]

		hPPARγ			mPPARγ			zfPPARγ			xPPARγ		
NR/chemical		% max act	EC_{20} (nM)	EC_{50} (nM)	% max act	EC_{20} (nM)	EC_{50} (nM)	% max act	EC_{20} (nM)	EC_{50} (nM)	% max act	EC_{20} (nM)	EC_{50} (nM)
	DMSO	15 ± 5			25 ± 6			8 ± 1			10 ± 2		
Ligands													
ligands of hPPARγ	rosiglitazone	100 ± 0	9.2 ± 0.7	24 ± 1.1	100 ± 0	5.5 ± 0.6	16 ± 1.1		NA		100 ± 0	197 ± 31	718 ± 100
	ciglitazone	77 ± 7	616 ± 19	1971 ± 81	71 ± 3	725 ± 130	2274 ± 618		NA		46 ± 0	1697 ± 24	4348 ± 129
	pioglitazone	111 ± 8	57 ± 7.3	259 ± 52	102 ± 1	54 ± 4.0	164 ± 24		NA		79 ± 6	889 ± 48	3627 ± 434
	troglitazone	114 ± 4	94 ± 11	232 ± 24	100 ± 8	98 ± 14	361 ± 87		NA		73 ± 4	837 ± 94	2312 ± 262
	GW 1929	85 ± 2	0.6 ± 0.05	1.8 ± 0.1	85 ± 6	0.7 ± 0.1	1.8 ± 0.2		NA		81 ± 3	69 ± 4.5	199 ± 10
	clofibric acid	39 ± 1	5065 ± 437	nd	38 ± 1	13 802 ± 1811	nd		NA		32 ± 7	7580 ± 1884	nd
	SR 1664	33 ± 1	129 ± 11	nd	33 ± 2	132 ± 20	nd		NA			NA	
	GW 9662*		NA			NA			NA		41 ± 1	0.2 ± 0.05	1.0 ± 0.1
	T0070907*	1 ± 0		inv.ago.	2 ± 1		inv.ago.		NA		49 ± 4	0.3 ± 0.1	2.0 ± 0.6
	SR 16832*	74 ± 2	0.1 ± 0.02	0.3 ± 0.03	61 ± 6	0.1 ± 0.02	0.7 ± 0.1		NA		61 ± 3	0.2 ± 0.1	1.0 ± 0.1
ligands of LXR	GW 3965	38 ± 8	4631 ± 424	nd		NA		100 ± 0	1033 ± 11	1849 ± 17	36 ± 5	6737 ± 487	nd
	T0901317		NA			NA			NA			NA	
	WAY-252623		NA			NA		114 ± 9	1542 ± 15	2759 ± 20		NA	
	GSK 2033*		NA			NA			NA			NA	
	SR 9238*		NA			NA			NA			NA	
	SR 9243*		NA			NA			NA			NA	
ligands of hPPARα	GW 7647	106 ± 0	121 ± 8.0	459 ± 36	97 ± 2	129 ± 14	518 ± 58		NA		85 ± 6	90 ± 11	381 ± 31
	CP 775,146	65 ± 6	507 ± 64	1986 ± 200	78 ± 2	903 ± 86	3682 ± 455	100 ± 8	3968 ± 378	6754 ± 421	68 ± 6	782 ± 89	3115 ± 349
	GW 6471*	4 ± 1		inv. ago.	8 ± 4		inv. ago.		NA		5 ± 0		inv. ago.

[a]Maximal activities are expressed as a percentage of the maximal luciferase activity induced by 1 μM rosiglitazone (HG5LN-hPPARγ, HG5LN-mPPARγ), 10 μM GW 3965 (HG5LN-zfPPARγ), or 10 μM rosiglitazone (HG5LN-xPPARγ). [b]NA: nonactive; nd: not determined; *: known antagonistic ligands; EC_{50}: half-maximal effective concentration; inv. ago.: inverse agonist.

https://doi.org/10.1021/acs.est.1c04318
Environ. Sci. Technol. 2021, 55, 16489−16501

Table 2. Minimal Activity and Half-Maximal Inhibitory Concentration (IC_{50}) of the Pharmaceuticals and Synthetic Ligands on h, m, zf, and xPPARγ[a,b]

		hPPARγ			mPPARγ			zfPPARγ			xPPARγ		
NR/chemical		% min act	IC_{20} (nM)	IC_{50} (nM)	% min act	IC_{20} (nM)	IC_{50} (nM)	% min act	IC_{20} (nM)	IC_{50} (nM)	% min act	IC_{20} (nM)	IC_{50} (nM)
	DMSO	70 ± 5			70 ± 6			75 ± 5			75 ± 5		
Ligands													
ligands of hPPARγ	rosiglitazone		NA			NA			NA			NA	
	ciglitazone		NA			NA			NA			NA	
	pioglitazone		NA			NA			NA			NA	
	troglitazone		NA			NA			NA			NA	
	GW 1929		NA			NA			NA			NA	
	clofibric acid		NA			NA			NA			NA	
	SR 1664	32 ± 6	815 ± 50	2505 ± 53	30 ± 5	602 ± 54	1989 ± 64	54 ± 3	2730 ± 124	5912 ± 495	37 ± 6	1578 ± 103	2808 ± 61
	GW 9662*	14 ± 1	2.7 ± 0.5	8.1 ± 1.0	23 ± 3	1.2 ± 0.1	4.9 ± 0.2		NA		42 ± 2	1.2 ± 0.4	3.9 ± 0.5
	T0070907*	3 ± 0	0.5 ± 0.02	1.5 ± 0.1	4 ± 0	0.6 ± 0.03	1.7 ± 0.2		NA		40 ± 3	1.0 ± 0.2	3.3 ± 0.4
	SR 16832*		NA			NA			NA		52 ± 0	0.6 ± 0.2	2.6 ± 0.5
ligands of LXR	GW 3965		NA			NA			NA			NA	
	T0901317		NA			NA			NA			NA	
	WAY-252623		NA			NA			NA			NA	
	GSK 2033*		NA			NA			NA			NA	
	SR 9238*		NA			NA			NA			NA	
	SR 9243*		NA			NA			NA			NA	
ligands of hPPARα	GW 7647		NA			NA			NA			NA	
	CP 775,146		NA			NA			NA			NA	
	GW 6471*	6 ± 3	77 ± 1.7	227 ± 40	9 ± 2	49 ± 7.2	138 ± 26		NA		45 ± 5	1436 ± 165	3853 ± 504

[a]Minimal activities are expressed as a percentage of the maximal luciferase activity induced by 1 μM rosiglitazone (HG5LN-hPPARγ, HG5LN-mPPARγ), 10 μM GW 3965 (HG5LN-zfPPARγ), or 10 μM rosiglitazone (HG5LN-xPPARγ). Molecules were coexposed with the reference ligand at 30 nM rosiglitazone (HG5LN-hPPARγ, HG5LN-mPPARγ), 2.6 μM GW 3965 (HG5LN-zfPPARγ), or 2 μM rosiglitazone (HG5LN-xPPARγ). [b]NA: nonactive; *: known antagonistic ligands; IC_{50}: half-maximal inhibitory concentration.

https://doi.org/10.1021/acs.est.1c04318
Environ. Sci. Technol. 2021, 55, 16489−16501

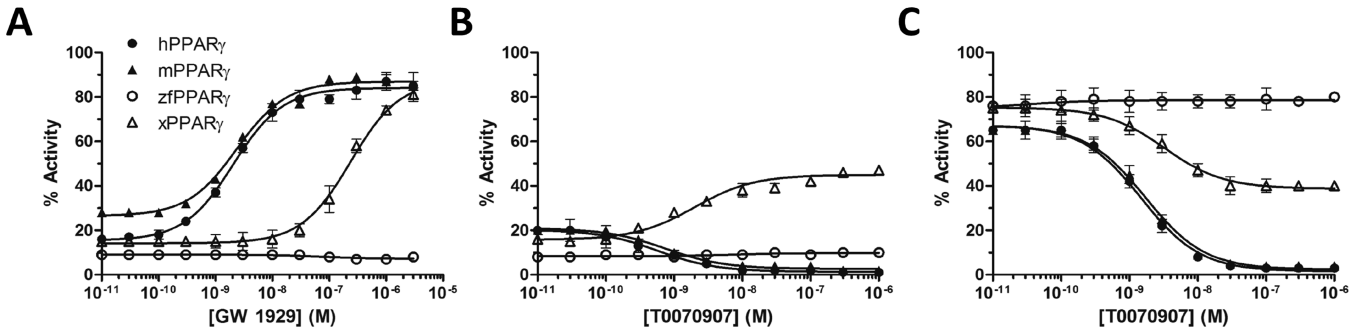

Figure 3. Transcriptional activity of h, m, zf, and xPPARγ in response to synthetic hPPARγ ligands. Results are expressed as a percentage of the maximum luciferase activity induced by 1 μM rosiglitazone (HG5LN-hPPARγ, HG5LN-mPPARγ), 10 μM GW 3965 (HG5LN-zfPPARγ), or 10 μM rosiglitazone (HG5LN-xPPARγ). GW 1929 (A) was tested in agonist assays; T0070907 was tested in agonist (B) and antagonist (C) assays. Error bars represent standard deviations.

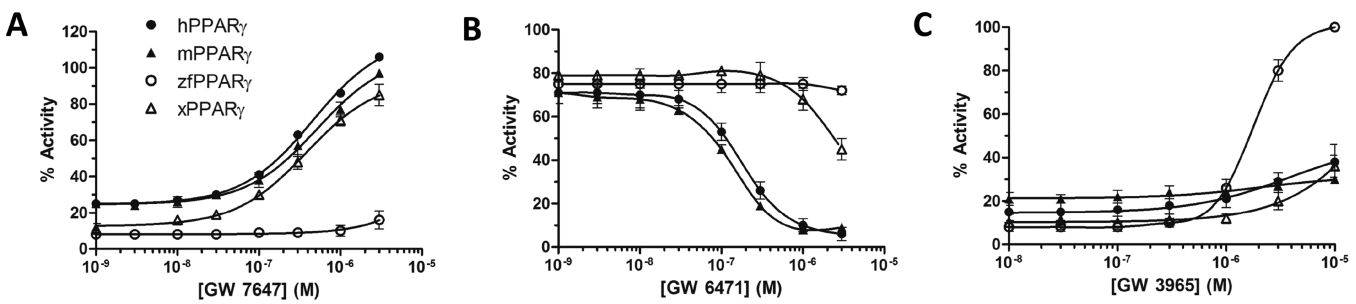

Figure 4. Transcriptional activity of h, m, zf, and xPPARγ in response to synthetic hPPARα and hLXR ligands. Results are expressed as a percentage of the maximum luciferase activity induced by 1 μM rosiglitazone (HG5LN-hPPARγ, HG5LN-mPPARγ), 10 μM GW 3965 (HG5LN-zfPPARγ), or 10 μM rosiglitazone (HG5LN-xPPARγ). Agonist hPPARα ligand GW 7647 (A) tested in agonist assay; antagonist hPPARα ligand GW 6471 (B) tested in antagonist assay; and agonist hLXR ligand GW 3965 tested in agonist assays (C). Error bars represent standard deviations.

All of these results highlighted major interspecies differences, notably that zfPPARγ is not activated nor inhibited by synthetic hPPARγ ligands.

Interspecies PPARγ Activity of Synthetic Ligands of hPPARα and hLXRs. As previously shown that the hPPARα ligand GW 7647 was active on hPPARγ,[21] we screened it and two other hPPARα synthetic chemicals to assess their activity on the four PPARγ. GW 7647 was able to activate the hPPARγ, mPPARγ, and xPPARγ with EC_{50} in the 100 nM range and very high efficiencies but did not modulate zfPPARγ activity (Figure 4A and Table 1). Another known ligand of hPPARγ, CP 775,146, transactivated these three receptors with lower potencies and efficacies, but more importantly transactivated zfPPARγ up to 100%, although with a relatively high EC_{50} of 6.8 μM (Table 1). The hPPARγ antagonist GW 6471 was able to downregulate the basal luminescence activity in HG5LN-hPPARγ, HG5LN-mPPARγ, and HG5LN-xPPARγ cells (data not shown), and in antagonist assays had IC_{50} in the 100 nM range for hPPARγ and mPPARγ and in the μM range for xPPARγ, thus acting as an inverse agonist (Figure 4B and Table 2).

To assess other potential interspecies differences and to find ligands that are able to regulate zfPPARγ activity, we also tested six known human liver X receptor (hLXR) synthetic ligands, as we previously observed that the hLXR ligand GW 3965 was able to activate zfPPARγ.[25] The hLXR ligand GW 3965 activated zfPPARγ with an EC_{50} of 1.8 μM (Figure 4C and Table 1) and was therefore used as the reference ligand in HG5LN-zfPPARγ cell line with a maximum luciferase activity reached at 10 μM. GW 3965 was also able to activate zfLXR as seen in the reporter cell line HG5LN-zfLXR cells (Pinto et al., 2016 and Supplementary Figure 2). The hLXR agonist WAY-252623, an anticholesterolemic chemical, transactivated zfPPARγ in a similar manner with an EC_{50} of 2.8 μM (Table 1). Another anticholesterolemic chemical agonist of the hLXR, T0901317, had no agonistic nor antagonistic effect on neither of PPARγs, as already described (Table 1 and Pinto et al., 2016). The hLXR antagonists GSK 2033, SR 9238, and SR 9243 had no effect on PPARγ activity either (Tables 1 and 2).

In conclusion, among the tested synthetic chemicals, only the hLXR ligands GW 3965 and WAY-252623 and the hPPARα ligand CP 775,146 were zfPPARγ agonists. Contrary to zfPPARγg, mPPARγ responded very similarly to hPPARγ to these chemicals, while xPPARγ had an intermediary profile as it was modulated by the same compounds but with lower potencies overall.

Interspecies PPARγ Activities of Environmental Chemicals. A selection of 21 chemicals that had been detected in the environment were tested on our models to assess potential interspecies differences, among which were nonsteroidal anti-inflammatory drugs (NSAIDs) (aspirin, diclofenac, ibuprofen, and indomethacin), an analgesic (acetaminophen), phthalates (BBP, DBP, MEHP), perfluorinated compounds (PFHexA, PFHepA, PFOA, PFNA, PFDA, PFunDA, PFOS), halogenated derivatives of BPA (TBBPA, TCBPA), and organophosphorus compounds (tri-*o*-tolyl phosphate, tri-*m*-tolyl phosphate, tri-*p*-tolyl phosphate, and triphenyl phosphate).

As some of these compounds, such as TBBPA, can strongly bind proteins present in the serum of the culture medium and can activate NRs (including PPARs) at relatively high concentrations with EC_{50} in the μM range,[26,27] we performed

https://doi.org/10.1021/acs.est.1c04318
Environ. Sci. Technol. 2021, 55, 16489−16501

Table 3. Maximal Activity and Half-Maximal Effective Concentration (EC_{50}) of the Environmental Chemicals on h, m, zf, and xPPARγ[a,b]

		hPPARγ			mPPARγ			zfPPARγ			xPPARγ		
NR/chemical		% max act	EC_{20} (μM)	EC_{50} (μM)	% max act	EC_{20} (μM)	EC_{50} (μM)	% max act	EC_{20} (μM)	EC_{50} (μM)	% max act	EC_{20} (μM)	EC_{50} (μM)
	DMSO	11 ± 4			15 ± 11			6 ± 2			8 ± 1		
Ligands													
environmental ligands	acetaminophen		NA			NA			NA			NA	
	aspirin		NA			NA			NA			NA	
	diclofenac		NA			NA		56 ± 9	1.4 ± 0.03	6.1 ± 2.5	56 ± 4	0.7 ± 0.1	2.2 ± 0.6
	ibuprofen	69 ± 3	22 ± 10	205 ± 80	62 ± 2	34 ± 2.0	238 ± 26		NA		58 ± 7	49 ± 9.1	128 ± 31
	indomethacin	120 ± 7	1.8 ± 0.1	6.2 ± 0.6	83 ± 10	2.7 ± 0.2	8.2 ± 1.4	95 ± 7	12 ± 0.5	53 ± 13	145 ± 6	3.8 ± 0.5	15 ± 1.5
	BBP	40 ± 3	2.0 ± 0.04	6.5 ± 1.9	38 ± 4	1.4 ± 0.3	nd	21 ± 1		nd	48 ± 4	3.8 ± 0.2	17 ± 5.8
	DBP	33 ± 5	1.9 ± 0.4	nd	41 ± 7	1.4 ± 0.3	nd	48 ± 6	14 ± 0.8	35 ± 1.6	47 ± 9	2.3 ± 0.4	13 ± 5.3
	MEHP	55 ± 8	4.8 ± 0.7	18 ± 0.9	45 ± 3	6.8 ± 1.7	24 ± 1.9	55 ± 8	11 ± 0.8	30 ± 1.4	66 ± 5	1.2 ± 0.1	4.6 ± 0.5
	PFHexA		NA			NA			NA			NA	
	PFHepA	38 ± 1		nd	39 ± 3		nd		NA		26 ± 4		nd
	PFOA	51 ± 3	17 ± 1.4	91 ± 12	57 ± 2	33 ± 6.2	545 ± 219	33 ± 7	73 ± 2.2	nd	53 ± 10	20 ± 1.1	217 ± 111
	PFNA	35 ± 5	24 ± 0.2	nd	30 ± 2	32 ± 2.6	nd	12 ± 3		nd	53 ± 6	17 ± 1.0	42 ± 11
	PFDA	23 ± 3		nd	44 ± 6		nd	18 ± 6		nd	28 ± 4		nd
	PFunDa		NA			NA		36 ± 10	4.8 ± 0.4	30 ± 13	26 ± 12	4.2 ± 2.0	10 ± 8.3
	PFOS	36 ± 4	21 ± 1.9	nd	52 ± 8	16 ± 2.0	67 ± 4.9	22 ± 10		nd	36 ± 6	23 ± 1.6	nd
	TBBPA	40 ± 4	0.1 ± 0.03	0.2 ± 0.1	26 ± 8	0.02 ± 0.01	0.1 ± 0.02	29 ± 3	0.5 ± 0.1	3.2 ± 1.8	22 ± 3	0.9 ± 0.6	19 ± 31
	TCBPA	47 ± 5	0.1 ± 0.04	0.3 ± 0.1	30 ± 4	0.1 ± 0.03	0.5 ± 0.1	20 ± 2	16 ± 0.8	69 ± 46	37 ± 2	1.1 ± 0.1	4.5 ± 0.8
	ToTP		NA			NA		77 ± 5	2.4 ± 0.1	5.3 ± 0.3		NA	
	TmTP	53 ± 9	0.8 ± 0.2	3.4 ± 1.0	33 ± 6	0.7 ± 0.4	nd	30 ± 7	2.2 ± 0.4	nd	32 ± 3	1.4 ± 0.2	nd
	TpTP	36 ± 5		nd	29 ± 1		nd	18 ± 7		nd	20 ± 2		nd
	TPP	28 ± 2		nd	24 ± 6		nd	104 ± 9	2.3 ± 0.02	3.5 ± 0.02	21 ± 4		nd

[a]Maximal activities are expressed as a percentage of the maximal luciferase activity induced by 1 μM rosiglitazone (HG5LN-hPPARγ, HG5LN-mPPARγ), 3 μM GW 3965 (HG5LN-zfPPARγ), or 10 μM rosiglitazone (HG5LN-xPPARγ). Compounds were tested without serum. [b]NA: nonactive; nd: not determined; EC_{50}: half-maximal effective concentration.

https://doi.org/10.1021/acs.est.1c04318
Environ. Sci. Technol. 2021, 55, 16489−16501

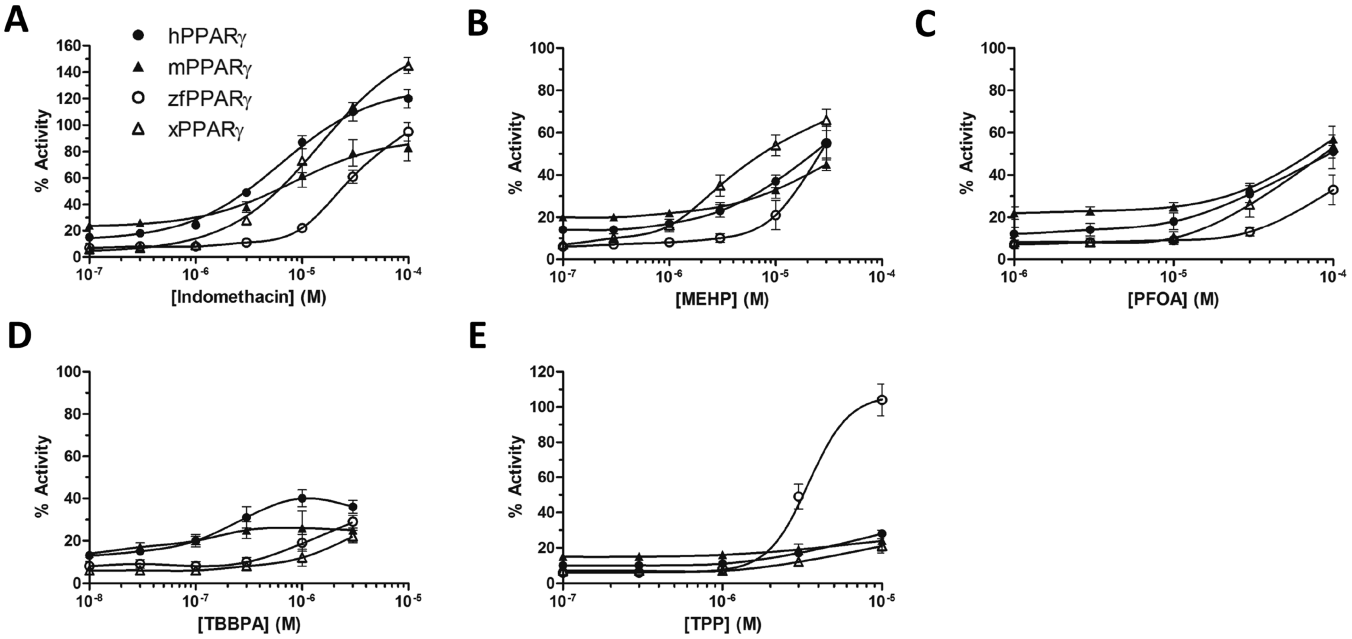

Figure 5. Transcriptional activity of h, m, zf, and xPPARγ in response to environmental compounds. Results are expressed as a percentage of the maximum luciferase activity induced by 1 μM rosiglitazone (HG5LN-hPPARγ, HG5LN-mPPARγ), 3 μM GW 3965 (HG5LN-zfPPARγ), or 10 μM rosiglitazone (HG5LN-xPPARγ). Compounds were tested without serum. Error bars represent standard deviations.

the assays in the absence of serum. First, we tested rosiglitazone, GW 3965, and TBBPA on hPPARγ and zfPPARγ with or without serum and showed that they were between 3 and 17 times more potent in the absence of serum (Supplementary Figure 3).

Among the antalgic compounds, acetaminophen and aspirin were not active in any of the receptors (Table 3).

Indomethacin was able to transactivate the four PPARγs with a lower potency for zfPPARγ (Figure 5A and Table 3). Ibuprofen activated hPPARγ, mPPARγ, and xPPARγ with EC_{50} in the 100 μM range and maximum up to 69% but did not activate zfPPARγ. These results on hPPARγ are in line with the literature.[28,29] According to these papers, indomethacin and ibuprofen induced adipocyte differentiation of murine preadipocytes. Diclofenac upregulated luciferase activity in zfPPARγ and xPPARγ cells (56% at 10 μM for both) but not in human and mouse models (Table 3). In the literature, diclofenac was described as a partial agonist of hPPARγ, although with weak efficacy.[29]

Three phthalates were tested on our cell lines, i.e., benzyl butyl phthalate (BBP), dibutyl phthalate (DBP), and phthalic acid mono-2-ethylhexyl ester (MEHP). As already described,[18,22] both BBP and MEHP were able to transactivate the human and zebrafish receptors. This was also the case for DBP. In addition, all three phthalates were active as well in mouse and xenopus models (Figure 5B and Table 3).

A selection of seven perfluorinated compounds was also tested in our models. This group of compounds are present worldwide in the environment due to their persistence, and bioaccumulative properties have already been identified as hPPARγ agonists.[30,31] Among them, PFHexA was not active in our cell lines, while PFHepA slightly upregulated luciferase activity in human, mouse, and xenopus models but not zebrafish. PFOA, PFNA, PFDA, and PFOS were active in all cell lines, while PFunDA was active only on the zebrafish and xenopus models (Figure 5C and Table 3). The different chain lengths and functional groups of the tested perfluorinated compounds indicate that perfluorinated compounds with chain lengths (C8−C10) tended to be more active than those with shorter or longer chain lengths, and the compounds with a sulfonate group were potentially more toxic than those with a carboxyl group.[32]

The two halogenated derivatives of BPA, TBBPA, and TCBPA (bromine or chlorine substituents of the phenolic rings, respectively), were tested in our models. They are used as flame retardants and their presence has been reported in the environment.[33−35] They were active in all of our models and had the lowest EC_{20s} among the environmental compounds we tested (from 0.02 μM) (Figure 5D and Table 3). These results concur with the literature as these compounds were also described as being active in human, zebrafish, and xenopus models in several studies.[18,22,27,36−38]

Finally, organophosphorus compounds used as flame retardants and plasticizers tri-*o*-tolyl phosphate (ToTP), tri-*m*-tolyl phosphate (TmTP), tri-*p*-tolyl phosphate (TpTP), and triphenyl phosphate (TPP) were tested in our models. TmTP, TpTP, and TPP transactivated the hPPARγ, mPPARγ, xPPARγ, and zfPPARγ, while ToTP only activated zPPARγ. Especially, ToTP and TPP transactivated zfPPARγ with high efficacies of 77 and 104%, respectively (Figure 5E and Table 3). TPP was also found to be active on h, m, and zfPPARγ *in vitro* by Houck et al., 2021 with EC_{50} in the same μM range.[39]

As opposed to the previous synthetic chemicals, most of the environmental compounds we tested were able to transactivate the zPPARγ, with profiles mostly similar to that of hPPARγ, which makes the use of this model relevant for hazard and risk assessment of environmental chemicals.

Molecular Modeling of hPPARγ, xPPARγ, and zfPPARγ to Explain Interaction Differences. To gain structural insights into the differential binding specificity of the PPARγ species, we used the server EDMon[40,41] to generate 3D models of zfPPARγ and xPPARγ LBDs. The sequence alignment of human, xenopus, and zebrafish PPARγ is shown in Supplementary Figure 4. These models were then compared

https://doi.org/10.1021/acs.est.1c04318
Environ. Sci. Technol. 2021, 55, 16489−16501

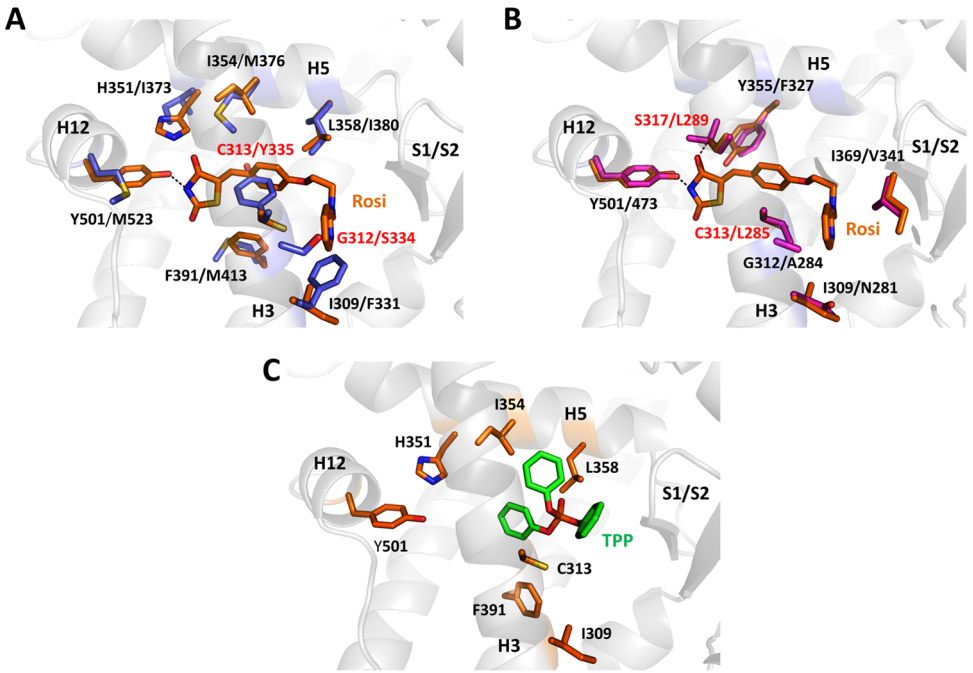

Figure 6. Structural basis for differential ligand-binding specificities of h, x, and zfPPARγ. (A) Rosiglitazone is positioned in the ligand-binding pocket of hPPARγ (crystal structure PDB code 2PRG). Residues that differ in the ligand-binding pockets of hPPARγ (orange) and zfPPARγ (blue) are displayed and labeled. The zebrafish receptor was modeled using the server EDMon (http://edmon.cbs.cnrs.fr). hPPARγ G312 and C313, which are replaced by serine and tyrosine residues, respectively, in the zebrafish receptor, are highlighted with red labels. (B) Superposition of the crystal structure of hPPARγ (2PRG) bound to rosiglitazone and a model of xPPARγ generated by the server EDMon. Residues that differ in the ligand-binding pockets of hPPARγ (orange) and xPPARγ (magenta) are displayed and labeled (except the tyrosine residue in helix H12, which is conserved in both species). hPPARγ C313 and S317, which are replaced by leucine residues in the xenopus receptor, are highlighted with red labels. (C) TPP as modeled in the ligand-binding pocket of hPPARγ.

to the experimental crystal structure of hPPARγ bound to rosiglitazone. The superimposition of zfPPARγ (Figure 6A) and xPPARγ (Figure 6B) on rosiglitazone-bound hPPARγ reveals residue differences, which certainly account for the specific response of each receptor to the various compounds. We first observed that, as compared to xPPARγ (residues shown in magenta in Figure 6B), the residues lining the ligand-binding pocket (LBP) of zfPPARγ (residues shown in blue in Figure 6A) differ significantly more from those of hPPARγ LBP (residues shown in orange in Figure 6A,B), both quantitatively and qualitatively.

This is consistent with cell-based[27] and *in vivo*[18] assays showing that, on average, the responsiveness to chemicals of zfPPARγ diverges more from that of hPPARγ than of xPPARγ. In particular, the replacement of hPPARγ G312 and C313 by bulkier serine and tyrosine residues in zfPPARγ generates steric clashes with the ligand and provides a rationale for the incapability of the zebrafish receptor to accommodate rosiglitazone (Figure 6A) and the other pharmaceuticals. In contrast, no such drastic steric hindrance exists in xPPARγ where the two main differences affecting rosiglitazone binding are the replacement of hPPARγ C313 and S317 by two leucine residues (Figure 6B). In addition to the bulkiness of leucine residues compared to that of C313 and S317, which most likely plays a role, it appears that the loss of the hydrogen bond between S317 (hPPARγ) and rosiglitazone (red dashed line in Figure 6B) is another key factor to explain why the pharmaceutical binds less avidly to xPPARγ than to hPPARγ.

We then used the program EDMon to predict the binding mode of the LXR agonist GW 3965 to zfPPARγ and hPPARγ (Supplementary Figure 5). The proposed binding modes are radically different from that of rosiglitazone in hPPARγ. The EDMon server predicts that, although GW 3935 adopts different positions in the two receptor species, it occupies the same subpocket located between helices H3, H5, and the β-sheet S1/S2 and makes no contact at all with the activation helix H12. This interaction is known to be a major determinant of ligand affinity and activity in hPPARγ, as illustrated with rosiglitazone in Figure 6A. In full agreement with this, GW 3935 is unable to bind and/or activate mPPARγ and xPPARγ, which also harbor a tyrosine residue in helix H12. Because the hPPARγ H12 Y473 polar residue is replaced with a hydrophobic methionine in zfPPARγ, a direct contact between the activation helix and the bound ligand might not be mandatory for activation of the zebrafish receptor.

We also used the program EDMon to predict the binding mode of the small compound TPP to hPPARγ. It predicted that TPP occupies the same subpocket as GW 3965 located between helices H3, H5, and the β-sheet S1/S2 (Figure 6C). Both the chemical composition of TPP and its predicted binding mode also preclude any contact with the activation helix H12 through the formation of a hydrogen bond with Y501, as exemplified with rosiglitazone (Figure 6A). In contrast, TPP could bind to and activate zfPPARγ. Together, the GW 3965 and TPP data suggest that a direct contact between H12 and the bound ligand might not be mandatory for activation of the zebrafish receptor.

Our results show that several synthetic compounds (GW 3965, WAY-252623) can affect wildlife through the disruption of the zfPPARγ pathway, in a way that is not necessarily predictable by the use of human or mouse assays. Conversely, results obtained in zebrafish models must be used with

https://doi.org/10.1021/acs.est.1c04318
Environ. Sci. Technol. 2021, 55, 16489−16501

precaution for assessing the hazard and risk of chemicals to human health. In this regard, our cell lines can be used for screening chemical substances to minimize the cost and use of animals in future studies, in accordance with the 3Rs principles (replacement, reduction and refinement). Previous studies investigating interspecies differences, notably between mammalian and nonmammalian species, have revealed variations in binding affinities or transactivation profiles for ERs,[42,43] PXR,[44−46] and PR[47] linked to essential residue differences in the LBD and strongly support the development and use of species-specific *in vitro* assays for the study of nuclear receptors.

■ ASSOCIATED CONTENT

Supporting Information

The Supporting Information is available free of charge at https://pubs.acs.org/doi/10.1021/acs.est.1c04318.

Luciferase activity of HG5LN in response to different concentrations of chemical substances (Supplementary Figure 1); transcriptional activity of hLXRα, hLXRβ, and zfLXR in response to GW 3965 (Supplementary Figure 2); transcriptional activity of hPPARγ and zfPPARγ in response to rosiglitazone, GW 3965, and TBBPA in culture medium with or without serum (Supplementary Figure 3); sequence alignment of human, xenopus, and zebrafish PPARγ ligand-binding pocket residues. Asterisks denote residues that are similar between the three species (Supplementary Figure 4); structural basis for differential GW 3965-binding specificity of h and zfPPARγ (Supplementary Figure 5); chemical substances used in this study (Supplementary Table 1); maximal activity and half-maximal effective concentration (EC_{50}) of GW 3965 on hLXRα, hLXRβ, and zfLXR (Supplementary Table 2); and maximal activity and half-maximal effective concentration (EC_{50}) of rosiglitazone, GW 3965, and TBBPA on hPPARγ and zfPPARγ with or without serum (Supplementary Table 3) (PDF)

■ AUTHOR INFORMATION

Corresponding Authors

Clémentine Garoche − *Institut de Recherche en Cancérologie de Montpellier (IRCM), Inserm U1194, Université Montpellier, Institut régional du Cancer de Montpellier (ICM), 34290 Montpellier, France;* orcid.org/0000-0002-9363-7945; Phone: +33(0)4 11 28 31 27; Email: clementine.garoche@inserm.fr

Patrick Balaguer − *Institut de Recherche en Cancérologie de Montpellier (IRCM), Inserm U1194, Université Montpellier, Institut régional du Cancer de Montpellier (ICM), 34290 Montpellier, France*; Phone: +33(0)4 11 28 31 27; Email: patrick.balaguer@inserm.fr

Authors

Abdelhay Boulahtouf − *Institut de Recherche en Cancérologie de Montpellier (IRCM), Inserm U1194, Université Montpellier, Institut régional du Cancer de Montpellier (ICM), 34290 Montpellier, France*

Marina Grimaldi − *Institut de Recherche en Cancérologie de Montpellier (IRCM), Inserm U1194, Université Montpellier, Institut régional du Cancer de Montpellier (ICM), 34290 Montpellier, France*

Barbara Chiavarina − *Institut de Recherche en Cancérologie de Montpellier (IRCM), Inserm U1194, Université Montpellier, Institut régional du Cancer de Montpellier (ICM), 34290 Montpellier, France*

Lucia Toporova − *Institut de Recherche en Cancérologie de Montpellier (IRCM), Inserm U1194, Université Montpellier, Institut régional du Cancer de Montpellier (ICM), 34290 Montpellier, France*

Marjo J. den Broeder − *Institute for Risk Assessment Sciences, Department of Population Health Sciences, Faculty of Veterinary Medicine, Utrecht University, 3584 CS Utrecht, The Netherlands*

Juliette Legler − *Institute for Risk Assessment Sciences, Department of Population Health Sciences, Faculty of Veterinary Medicine, Utrecht University, 3584 CS Utrecht, The Netherlands*

William Bourguet − *Centre de Biologie Structurale (CBS), Inserm U1053, CNRS, Université Montpellier, 34290 Montpellier, France*

Complete contact information is available at: https://pubs.acs.org/10.1021/acs.est.1c04318

Notes

The authors declare no competing financial interest.

■ ACKNOWLEDGMENTS

This research was supported by the ANR project SYNERACT, the ANSES project TOXCHEM, and the European Union's Horizon 2020 research and innovation programme under agreement No. 825489 (GOLIATH project).

■ ABBREVIATIONS

BBP	benzyl butyl phthalate
DBD	DNA-binding domain
DBP	dibutyl phthalate
DCC	dextran-coated charcoal
DMEM	Dulbecco's modified Eagle's medium
DMSO	dimethyl sulfoxide
EDCs	endocrine disrupting chemicals
h	human
LBD	ligand-binding domain
LXR	liver X receptor
m	mouse
MEHP	phthalic acid mono-2-ethylhexyl ester
NR	nuclear receptor
PFHexA	perfluorohexanoic acid
PFHepA	perfluoroheptanoic acid
PFOA	perfluorooctanoic acid
PFNA	perfluorononanoic acid
PFDA	perfluorodecanoic acid
PFunDA	perfluoroundecanoic acid
PFOS	heptadecafluorooctane sulfonic acid
PPAR	peroxisome proliferator-activated receptor
PPREs	peroxisome proliferator response elements
RXR	retinoid X receptor
TBBPA	tetrabromobisphenol A
TCBPA	tetrachlorobisphenol A
ToTP	tri-*ortho*-tolyl phosphate
TmTP	tri-*meta*-tolyl phosphate
TpTP	tri-*para*-tolyl phosphate
TPP	triphenyl phosphate
x	xenopus

https://doi.org/10.1021/acs.est.1c04318
Environ. Sci. Technol. 2021, 55, 16489−16501

zf zebrafish

REFERENCES

(1) Issemann, I.; Green, S. Activation of a Member of the Steroid Hormone Receptor Superfamily by Peroxisome Proliferators. *Nature* **1990**, *347*, 645−650.

(2) Dreyer, C.; Krey, G.; Keller, H.; Givel, F.; Helftenbein, G.; Wahli, W. Control of the Peroxisomal β-Oxidation Pathway by a Novel Family of Nuclear Hormone Receptors. *Cell* **1992**, *68*, 879−887.

(3) Kliewer, S. A.; Forman, B. M.; Blumberg, B.; Ong, E. S.; Borgmeyer, U.; Mangelsdorf, D. J.; Umesono, K.; Evans, R. M. Differential Expression and Activation of a Family of Murine Peroxisome Proliferator-Activated Receptors. *Proc. Natl. Acad. Sci. U.S.A.* **1994**, *91*, 7355−7359.

(4) Latruffe, N.; Vamecq, J. Peroxisome Proliferators and Peroxisome Proliferator Activated Receptors (PPARs) as Regulators of Lipid Metabolism. *Biochimie* **1997**, *79*, 81−94.

(5) Tontonoz, P.; Hu, E.; Spiegelman, B. M. Stimulation of Adipogenesis in Fibroblasts by PPARγ2, a Lipid-Activated Transcription Factor. *Cell* **1994**, *79*, 1147−1156.

(6) Elbrecht, A.; Chen, Y.; Cullinan, C. A.; Hayes, N.; Leibowitz, M. D.; Moller, D. E.; Berger, J. Molecular Cloning, Expression and Characterization of Human Peroxisome Proliferator Activated Receptors Γ1 and Γ2. *Biochem. Biophys. Res. Commun.* **1996**, *224*, 431−437.

(7) Mukherjee, R.; Jow, L.; Croston, G. E.; Paterniti, J. R. Identification, Characterization, and Tissue Distribution of Human Peroxisome Proliferator-Activated Receptor (PPAR) Isoforms PPARγ2 versus PPARγ1 and Activation with Retinoid X Receptor Agonists and Antagonists. *J. Biol. Chem.* **1997**, *272*, 8071−8076.

(8) Kersten, S.; Mandard, S.; Tan, N. S.; Escher, P.; Metzger, D.; Chambon, P.; Gonzalez, F. J.; Desvergne, B.; Wahli, W. Characterization of the Fasting-Induced Adipose Factor FIAF, a Novel Peroxisome Proliferator-Activated Receptor Target Gene. *J. Biol. Chem.* **2000**, *275*, 28488−28493.

(9) Michalik, L.; Desvergne, B.; Wahli, W. Peroxisome-Proliferator-Activated Receptors and Cancers: Complex Stories. *Nat. Rev. Cancer* **2004**, 61−70.

(10) Sharma, A. M.; Staels, B. Review: Peroxisome Proliferator-Activated Receptor γ and Adipose Tissue - Understanding Obesity-Related Changes in Regulation of Lipid and Glucose Metabolism. *J. Clin. Endocrinol. Metab.* **2007**, 386−395.

(11) Lehmann, J. M.; Moore, L. B.; Smith-Oliver, T. A.; Wilkison, W. O.; Willson, T. M.; Kliewer, S. A. An Antidiabetic Thiazolidinedione Is a High Affinity Ligand for Peroxisome Proliferator-Activated Receptor γ (PPARγ). *J. Biol. Chem.* **1995**, *270*, 12953−12956.

(12) Yki-Järvinen, H. Thiazolidinediones. *N. Engl. J. Med.* **2004**, *351*, 1106−1118.

(13) Castillo, L.; Seriki, K.; Mateos, S.; Loire, N.; Guédon, N.; Lemkine, G. F.; Demeneix, B. A.; Tindall, A. J. In Vivo Endocrine Disruption Assessment of Wastewater Treatment Plant Effluents with Small Organisms. *Water Sci. Technol.* **2013**, *68*, 261−268.

(14) Dai, Y. J.; Jia, Y. F.; Chen, N.; Bian, W. P.; Li, Q. K.; Ma, Y. B.; Chen, Y. L.; Pei, D. S. Zebrafish as a Model System to Study Toxicology. *Environ. Toxicol. Chem.* **2014**, 11−17.

(15) Lee, O.; Green, J. M.; Tyler, C. R. Transgenic Fish Systems and Their Application in Ecotoxicology. *Crit. Rev. Toxicol.* **2015**, *45*, 124−141.

(16) Mughal, B. B.; Demeneix, B. A.; Fini, J. B. Evaluating Thyroid Disrupting Chemicals in Vivo Using Xenopus Laevis. In *Methods in Molecular Biology*; Humana Press Inc., 2018; Vol. *1801*, pp 183−192.

(17) Tiefenbach, J.; Moll, P. R.; Nelson, M. R.; Hu, C.; Baev, L.; Kislinger, T.; Krause, H. M. A Live Zebrafish-Based Screening System for Human Nuclear Receptor Ligand and Cofactor Discovery. *PLoS One* **2010**, *5*, No. e9797.

(18) Riu, A.; Mccollum, C. W.; Pinto, C. L.; Grimaldi, M.; Hillenweck, A.; Perdu, E.; Zalko, D.; Bernard, L.; Laudet, V.; Balaguer, P.; et al. Halogenated Bisphenol-A Analogs Act as Obesogens in Zebrafish Larvae (Danio Rerio). *Toxicol. Sci.* **2014**, *139*, 48−58.

(19) Den Broeder, M. J.; Kopylova, V. A.; Kamminga, L. M.; Legler, J. Zebrafish as a Model to Study the Role of Peroxisome Proliferating-Activated Receptors in Adipogenesis and Obesity. *PPAR Res.* **2015**, *2015*, No. 358029.

(20) den Broeder, M. J.; Moester, M. J. B.; Kamstra, J. H.; Cenijn, P. H.; Davidoiu, V.; Kamminga, L. M.; Ariese, F.; De Boer, J. F.; Legler, J. Altered Adipogenesis in Zebrafish Larvae Following High Fat Diet and Chemical Exposure Is Visualised by Stimulated Raman Scattering Microscopy. *Int. J. Mol. Sci.* **2017**, *18*, No. 894.

(21) Seimandi, M.; Lemaire, G.; Pillon, A.; Perrin, A.; Carlavan, I.; Voegel, J. J.; Vignon, F.; Nicolas, J. C.; Balaguer, P. Differential Responses of PPARα, PPARδ, and PPARγ Reporter Cell Lines to Selective PPAR Synthetic Ligands. *Anal. Biochem.* **2005**, *344*, 8−15.

(22) Grimaldi, M.; Boulahtouf, A.; Delfosse, V.; Thouennon, E.; Bourguet, W.; Balaguer, P. Reporter Cell Lines to Evaluate the Selectivity of Chemicals for Human and Zebrafish Estrogen and Peroxysome Proliferator Activated γ Receptors. *Front. Neurosci.* **2015**, *9*, No. 212.

(23) Lee, G.; Elwood, F.; Mcnally, J.; Weiszmann, J.; Lindstrom, M.; Amaral, K.; Nakamura, M.; Miao, S.; Cao, P.; Learned, R. M.; et al. T0070907, a Selective Ligand for Peroxisome Proliferator-Activated Receptor γ, Functions as an Antagonist of Biochemical and Cellular Activities. *J. Biol. Chem.* **2002**, *277*, 19649−19657.

(24) Choi, J. H.; Banks, A. S.; Kamenecka, T. M.; Busby, S. A.; Chalmers, M. J.; Kumar, N.; Kuruvilla, D. S.; Shin, Y.; He, Y.; Bruning, J. B.; et al. Antidiabetic Actions of a Non-Agonist PPARγ Ligand Blocking Cdk5-Mediated Phosphorylation. *Nature* **2011**, *477*, 477−481.

(25) Pinto, C. L.; Kalasekar, S. M.; McCollum, C. W.; Riu, A.; Jonsson, P.; Lopez, J.; Swindell, E. C.; Bouhlatouf, A.; Balaguer, P.; Bondesson, M.; et al. Lxr Regulates Lipid Metabolic and Visual Perception Pathways during Zebrafish Development. *Mol. Cell. Endocrinol.* **2016**, *419*, 29−43.

(26) Endo, S.; Goss, K.-U. Serum Albumin Binding of Structurally Diverse Neutral Organic Compounds: Data and Models. *Chem. Res. Toxicol.* **2011**, *24*, 2293−2301.

(27) Riu, A.; Grimaldi, M.; Maire, A.; Bey, G.; Phillips, K.; Boulahtouf, A.; et al. Peroxisome Proliferator-Activated Receptor γ Is a Target for Halogenated Analogs of Bisphenol A. *Environ. Health Perspect.* **2011**, *119*, 1227−1232.

(28) Lehmann, J. M.; Lenhard, J. M.; Oliver, B. B.; Ringold, G. M.; Kliewer, S. A. Peroxisome Proliferator-Activated Receptors α and γ Are Activated by Indomethacin and Other Non-Steroidal Anti-Inflammatory Drugs. *J. Biol. Chem.* **1997**, *272*, 3406−3410.

(29) Puhl, A. C.; Milton, F. A.; Cvoro, A.; Sieglaff, D. H.; Campos, J. C. L.; Filgueira, C. S.; Lindemann, J. L.; Deng, T.; Neves, F. A. R.; Polikarpov, I.; et al. Mechanisms of Peroxisome Proliferator Activated Receptor γ Regulation by Non-Steroidal Anti-Inflammatory Drugs. *Nucl. Recept. Signaling* **2015**, *13*, No. nrs.13004.

(30) Behr, A. C.; Plinsch, C.; Braeuning, A.; Buhrke, T. Activation of Human Nuclear Receptors by Perfluoroalkylated Substances (PFAS). *Toxicol. In Vitro* **2020**, *62*, No. 104700.

(31) Wolf, C.; Takacs, M.; Schmid, J.; Lau, C.; Abbott, B. Activation of Mouse and Human Peroxisome Proliferator-Activated Receptor Alpha by Perfluoroalkyl Acids of Different Functional Groups and Chain Lengths. *Toxicol. Sci.* **2008**, *106*, 162−171.

(32) Hagenaars, A.; Vergauwen, L.; De Coen, W.; Knapen, D. Structure-Activity Relationship Assessment of Four Perfluorinated Chemicals Using a Prolonged Zebrafish Early Life Stage Test. *Chemosphere* **2011**, *82*, 764−772.

(33) de Wit, C. A.; Herzke, D.; Vorkamp, K. Brominated Flame Retardants in the Arctic Environment - Trends and New Candidates. *Sci. Total Environ.* **2010**, *408*, 2885−2918.

(34) Darnerud, P. O. Toxic Effects of Brominated Flame Retardants in Man and in Wildlife. *Environ. Int.* **2003**, *29*, 841−853.

https://doi.org/10.1021/acs.est.1c04318
Environ. Sci. Technol. 2021, 55, 16489−16501

(35) Chu, S.; Haffner, G. D.; Letcher, R. J. Simultaneous Determination of Tetrabromobisphenol A, Tetrachlorobisphenol A, Bisphenol A and Other Halogenated Analogues in Sediment and Sludge by High Performance Liquid Chromatography-Electrospray Tandem Mass Spectrometry. *J. Chromatogr. A* **2005**, *1097*, 25−32.
(36) Grimaldi, M.; Boulahtouf, A.; Delfosse, V.; Thouennon, E.; Bourguet, W.; Balaguer, P. Reporter Cell Lines for the Characterization of the Interactions between Human Nuclear Receptors and Endocrine Disruptors. *Front. Endocrinol.* **2015**, *6*, No. 62.
(37) Riu, A.; Maire, A.; Grimaldi, M.; Audebert, M.; Hillenweck, A.; Bourguet, W.; Balaguer, P.; Zalko, D. Characterization of Novel Ligands of ERα, ERβ, and PPARγ: The Case of Halogenated Bisphenol A and Their Conjugated Metabolites. *Toxicol. Sci.* **2011**, *122*, 372−382.
(38) Kopp, R.; Martínez, I. O.; Legradi, J.; Legler, J. Exposure to Endocrine Disrupting Chemicals Perturbs Lipid Metabolism and Circadian Rhythms. *J. Environ. Sci.* **2017**, *62*, 133−137.
(39) Houck, K. A.; Simha, A.; Bone, A.; Doering, J. A.; Vliet, S. M. F.; LaLone, C.; Medvedev, A.; Makarov, S. Evaluation of a Multiplexed, Multispecies Nuclear Receptor Assay for Chemical Hazard Assessment. *Toxicol. In Vitro* **2021**, *72*, No. 105016.
(40) Schneider, M.; Pons, J.-L.; Bourguet, W.; Labesse, G. Towards Accurate High-Throughput Ligand Affinity Prediction by Exploiting Structural Ensembles, Docking Metrics and Ligand Similarity. *Bioinformatics* **2020**, *36*, 160−168.
(41) Schneider, M.; Pons, J. L.; Labesse, G.; Bourguet, W. In Silico Predictions of Endocrine Disruptors Properties. *Endocrinology* **2019**, 2709−2716.
(42) Pinto, C.; Grimaldi, M.; Boulahtouf, A.; Pakdel, F.; Brion, F.; Aït-Aïssa, S.; Cavaillès, V.; Bourguet, W.; Gustafsson, J. A.; Bondesson, M.; et al. Selectivity of Natural, Synthetic and Environmental Estrogens for Zebrafish Estrogen Receptors. *Toxicol. Appl. Pharmacol.* **2014**, *280*, 60−69.
(43) Pinto, C.; Hao, R.; Grimaldi, M.; Thrikawala, S.; Boulahtouf, A.; Aït-Aïssa, S.; Brion, F.; Gustafsson, J. Å.; Balaguer, P.; Bondesson, M. Differential Activity of BPA, BPAF and BPC on Zebrafish Estrogen Receptors in Vitro and in Vivo. *Toxicol. Appl. Pharmacol.* **2019**, *380*, No. 114709.
(44) Ekins, S.; Reschly, E. J.; Hagey, L. R.; Krasowski, M. D. Evolution of Pharmacologic Specificity in the Pregnane X Receptor. *BMC Evol. Biol.* **2008**, *8*, No. 103.
(45) Lange, A.; Corcoran, J.; Miyagawa, S.; Iguchi, T.; Winter, M. J.; Tyler, C. R. Development of a Common Carp (Cyprinus Carpio) Pregnane X Receptor (CPXR) Transactivation Reporter Assay and Its Activation by Azole Fungicides and Pharmaceutical Chemicals. *Toxicol. In Vitro* **2017**, *41*, 114−122.
(46) Zhao, Y.; Zhang, K.; Giesy, J. P.; Hu, J. Families of Nuclear Receptors in Vertebrate Models: Characteristic and Comparative Toxicological Perspective. *Sci. Rep.* **2015**, *5*, No. 8554.
(47) Garoche, C.; Aït-Aïssa, S.; Boulahtouf, A.; Creusot, N.; Hinfray, N.; Bourguet, W.; Balaguer, P.; Brion, F. Human and Zebrafish Nuclear Progesterone Receptors Are Differently Activated by Manifold Progestins. *Environ. Sci. Technol.* **2020**, *54*, 9510−9518.

https://doi.org/10.1021/acs.est.1c04318
Environ. Sci. Technol. 2021, 55, 16489−16501